PHYSICAL REVIEW B **82**, 201304(R) (2010)

Formation and vanishing of short range ordering in $GaAs_{1-x}Bi_x$ thin films

G. Ciatto,[1,*] M. Thomasset,[1] F. Glas,[2] X. Lu,[3] and T. Tiedje[3]
[1]*Synchrotron SOLEIL, L'Orme des Merisiers, Saint-Aubin, BP 48, 91192 Gif-sur-Yvette Cedex, France*
[2]*Laboratoire de Photonique et de Nanostructures, CNRS, Route de Nozay, 91460 Marcoussis, France*
[3]*Department of Physics and Astronomy, University of British Columbia, Vancouver, British Columbia, Canada V6T 1Z1*
(Received 17 August 2010; published 9 November 2010)

We address the compositional evolution of the structure of $GaAs_{1-x}Bi_x$ thin films at different scale lengths by combining x-ray absorption spectroscopy, atomic force microscopy, and x-ray diffraction. We find that Bi short range ordering, observed for $x<3\%$, drastically vanishes for $x\geq 5.4\%$. The recovery of random anion distribution goes along with the formation of Bi droplets at the sample surface while bulk maintains high crystalline quality. These structural changes go with the anomalous behavior of optical and electronic properties. In particular, we find that the decrease in emission intensity in the samples corresponds to the concentration point where Bi short range ordering is lost, hence the preservation of nonrandom distribution turns to be a key point in devices design.

DOI: 10.1103/PhysRevB.82.201304 PACS number(s): 61.05.cj, 68.35.Rh, 81.05.Ea, 88.40.jm

Research on renewable energy is becoming a priority in order to response to the challenges of reducing carbon emission and climate change. According to the statistics report of the International Energy Agency,[1] solar photovoltaics (PV) is one of the less exploited renewable energy sources, far from hydroelectric, wind, and geothermal. One of the major limitations to the large-scale development of PV is the low efficiency of classical silicon solar cells. In prototype multijunction solar cells[2,3] III-V semiconductors substitute Si and the choice of materials combination optimizing absorption and transport is essential. Recently, dilute bismides[4] emerged as promising candidates to be used in PV devices. The incorporation of heavy Bi anions causes an enormous redshift of the GaAs band gap,[5] which gives access to the most interesting energies in the infrared, and is predicted to induce localized levels around the valence-band maximum of GaAs (Ref. 6) instead of the conduction-band minimum (unlike in $GaAs_{1-x}N_x$) with beneficial effects on electrons carriers transport properties.[7] $GaAs_{1-x}Bi_x$ alloys, which have been grown up to $x=11\%$,[8] have encouraging room-temperature photoluminescence (PL) emission,[5] along with still unexplained anomalous optical and electronics properties: a giant optical bowing, a nonlinear behavior of PL intensity as a function of x,[5] and an intriguing trend of the exciton effective mass.[9]

In a recent work, we have studied the Bi local environment in $GaAs_{1-x}Bi_x$ epilayers at relatively low x (1.2–2.4 %) by x-ray absorption fine-structure spectroscopy (XAFS) and found that short range ordering (SRO) of Bi atoms, in form of Bi pairs and tetramers association over random statistics, takes place.[10] In this Rapid Communication we extend our analysis to a wider concentration range in order to establish a correlation between the local structural properties and the optical and electronic ones. As a matter of fact, in a III-V alloy, when the substitution of a small fraction of atoms with isovalent ones produces impurity levels which are close to the host band edges, the electronic structure, and optical band gap can be strongly dependent on the deviation from random distribution of the impurities, as it has been recently predicted in the case of $GaSb_{1-x}N_x$.[11] Therefore, we expect a similar effect for the case of $GaAs_{1-x}Bi_x$.

We measured three 38-nm-thick $GaAs_{1-x}Bi_x$ films grown by molecular-beam epitaxy on GaAs substrate with $x=5.4\%$, 8.2%, and 10.9%. The detailed growth procedure was described elsewhere.[8] We also measured a thicker epilayer (360 nm) with $x=7\%$ and a metallic Bi foil in the same experimental conditions. Sample concentration was obtained by x-ray diffraction (XRD). XAFS was performed at liquid nitrogen temperature at the BM29 beamline of the European Synchrotron Radiation Facility (ESRF), adopting an experimental setup identical to the one used in our previous experiment.[10] Figure 1 shows the Fourier transform (FT) of Bi-L2 XAFS spectra for the samples referred above plus two epilayers with $x=1.2\%$ and 2.4% measured in our previous work[10] and the metallic Bi foil. Comparing the $x=5.4\%$ sample with the $x=2.4\%$ one, we observe an astonishing decrease in the FT amplitude. Increasing x again, the first shell peak (which abscissa at 2.2 Å is related to the Bi near-

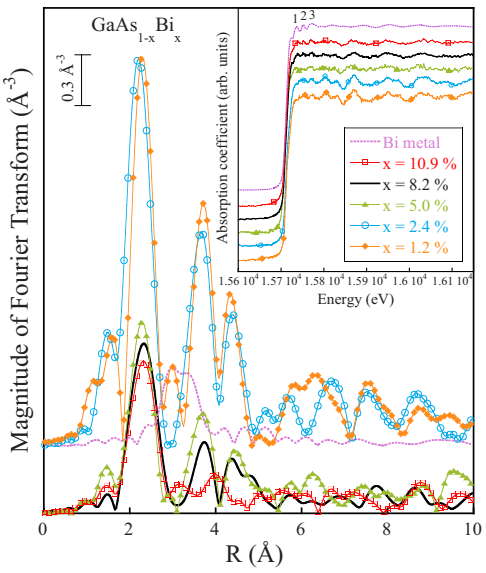

FIG. 1. (Color online) Bi L_2-edge XAFS Fourier transform of the three samples under study plus two samples from our previous paper (Ref. 10). Inset: normalized XAFS spectra.

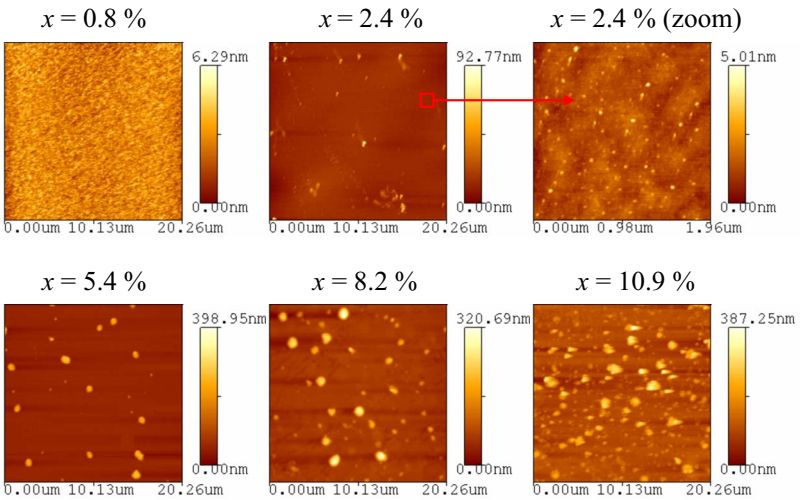

FIG. 2. (Color online) AFM images of $GaAs_{1-x}Bi_x$ thin films.

est neighbors distance) decreases more gently. The FT amplitude of the thicker $x=7\%$ epilayer (not shown) does not follow the trend of the three 38 nm ones but lays between these and the one of the $x=2.4\%$ epilayer. This suggests that the origin of the amplitude decrease is related to the surface. The inset of Fig. 1 shows the normalized absorption coefficient of all samples. It is evident that fine-structure oscillations have larger amplitude for the $x=1.2\%$ and $x=2.4\%$ epilayers and are smoothed down in the other samples. Also, one can note that the spectrum of the Bi metal shows very smooth oscillations in the energy range $\geq 15\ 800$ eV. Eventually, in the spectra of the three high-x epilayers, three x-ray absorption near-edge structure (XANES) features (labeled as 1, 2, and 3) match the ones of the metallic foil while the $x=1.2\%$ and $x=2.4\%$ samples have a different XANES. This suggests that the high-x samples are a mixture of a zinc blende and a metallic phase.

It has been observed that Bi tends to segregate at the sample surface and that the conditions which optimize sample quality are very close to the ones for which Bi or Ga droplets form,[8] so we performed atomic force microscopy (AFM) in order to understand if the presence of Bi droplets can account for the metallic contamination of the samples suggested by XANES. AFM was performed in oscillation mode with a Pacific Nanotechnology instrument. Figure 2 shows the AFM images recorded for the samples under study and for a $x=0.8\%$ sample. A $20\times 20\ \mu m^2$ image taken on the latter sample reveals a smooth surface without any three-dimensional feature. When inspecting the surface of the $x=2.4\%$ epilayer on the same length scale, we observe irregularly shaped surface features with rather low density while the most of surface area looks flat; nevertheless a $2\times 2\ \mu m^2$ zoom on a flat region reveals the existence of small structures with average dimension on the order of few tens of nanometers. Quantitative treatment of the image allowed us to extract the volume fraction occupied by the nano-objects with respect to the smooth regions, which is about 1/1000 for this sample. By increasing the concentration to $x=5.4\%$, larger particles (on the order of 1 μm) of roughly spherical shape form; the density of these microstructures is still relatively low and the volumetric fraction occupied by the particles to the smooth part of the sample increases to about 1/10. Despite the presence of these microstructures, $2\times 2\ \mu m^2$ zooms performed on particle-free regions (not shown) unreveal a very smooth surface. When increasing x to 8.2%, the density and average dimension of the microstructures increase again, the volumetric ratio to the epilayer approaches 1/4, and the shape distribution becomes less regular. Finally, at $x=10.9\%$, large part of the surface area is covered with structures of irregular shape and size distribution, in this case the volume fraction occupied by such structures is comparable with the volume of the smooth regions.

These results open several questions: first, even if it may seem straightforward to associate the particles observed by AFM to the Bi droplets reported in previous studies,[8] one can argue that under this hypothesis the decrease in the FT amplitude as a function of x shown in Fig. 1 would not be a linear function of the droplets volumetric fraction. Moreover, in the most concentrated sample, since the surface microstructures/epilayer volume ratio is close to 1 while x is only =10.9% in the epilayer part of the sample, one would expect a XAFS spectrum totally dominated by the metallic component while this is clearly not true from Fig. 1 where the first shell of the semiconductor structure continues to produce the most intense FT peak. On the other hand, the concern of a degradation of the structural quality of the epilayer as a consequence of the highly damaged surface is ruled out by XRD rocking curves performed around the (004) GaAs crystal plane reflection, which show very clear interference fringes also for the highest concentrations (Fig. 3 inset). This observation assures the very good quality of the interface and the long-range order in the semiconductive part of the samples. The situation is even more puzzling if one considers that we did not find any signature of crystalline precipitates (either Bi or Ga) in XRD data (not shown), which leads us to think that droplets, despite their apparent size, are closer to the amorphous state than to the crystalline one. In order to understand these points, we performed quantitative analysis of the XAFS spectra. First, we ruled out the hypothesis that the FT amplitude decrease in the high-x samples can be simply accounted for by the distance distribution broadening due to the higher Bi concentration and/or to the presence of a Bi gradient since the observed damping

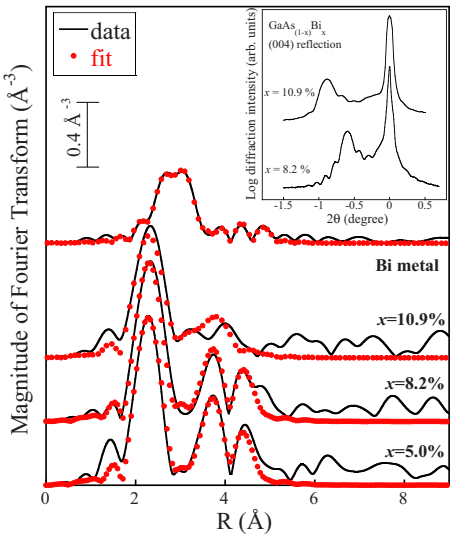

FIG. 3. (Color online) Fits on the FT of the XAFS signal for the samples under study plus the bulk Bi foil. In the inset: XRD rocking curve for the two samples with highest concentration.

is by far larger. On the contrary, we were able to well simulate the experimental data using the model of a mixture of a semiconductive and a metallic structure. As for the semiconductive part, we used the same analysis strategy reported previously and remind to the relative references for details.[10,12] The only change introduced was that, in order to compensate the small concentration difference between samples and supercells, we permitted one additional degree of freedom in the fit (ΔR): a common proportional variation in all distances, which can fluctuate around the values determined by our valence force-field minimization. As for the metallic part, in order to minimize the number of variables, we used the interatomic distances extracted from the fit of the Bi foil as fixed parameters while fitting the mixture. On the other hand, XRD indicates that the structure of a Bi droplet is more disordered compared to the one of a metallic foil, therefore in the fit of the mixture we introduced one more variable which multiplies the Debye-Waller (DW) factors extracted for the Bi foil. Results of the fits are shown in the body of Fig. 3, best fits are obtained by using a mixture of an ordered zinc-blende structure with random distribution of Bi atoms and a very disordered Bi metallic one, characterized by DW factors four times larger than the corresponding ones in the Bi foil. The Bi metallic fraction in the three 38 nm epilayers corresponds to roughly 50% and increases only slightly with x while it is 34% in the 360 nm epilayer. Metallic fractions and ΔR values extracted from the fits are reported in Table I along with the measured average number of Bi atoms in the second shell, its expected value in case of random anion distribution, and the ratio between the measured and expected value, which gives a SRO parameter describing the association of Bi anions in the V-group sublattice. As for SRO, data from our previous paper[10] on low-x samples are reported for comparison. We remark that the adopted analysis method allows us to separate the semiconductive part of the sample from the metallic one and to address the issue of Bi SRO in the $GaAs_{1-x}Bi_x$ epilayer even in case of strong perturbation of the surface, and that quality of the fits is very good but for the $x=10.9\%$ sample where we were not able to describe the second and third shells because of their very low amplitude. One could notice that a fourfold increase in DW factors relative to bulk crystalline material is rather large and closer to the value determined for 3 nm amorphous-metal nanoparticles[13] than to the one of micrometric structures. Even if DW factors of this magnitude have been already measured for Bi clusters larger than 20 nm (resulting from total reduction of bismuth-silicate glasses[14]) it is probable that our droplets (as preliminary high-resolution imaging suggests) are actually agglomerates of smaller nanosized precipitates. We verified, via full multiple-scattering simulations, that three atomic shells of the Bi metallic structure are sufficient to generate the features labeled as (1, 2, and 3) in Fig. 1 inset, and that a fourfold increase in DW factors brings about an amplitude reduction but not the disappearance of such features. Therefore our results are compatible with a quasiamorphous nature of the Bi droplets, which conserve some order (even if with very high DW factors) up to three atomic shells (i.e., in a subnanometric regime) but without any long-range order able to produce XRD peaks. Finally, we observe that the small ΔR measured by XAFS are in qualitative agreement with the values derivable from the XRD curves in Fig. 3 inset.

Figure 4 summarizes our main results: we plot here the SRO parameter and the relative amplitude of the XAFS FT first shell peak as a function of x. We find that Bi atoms association is over random statistics in the concentration range $x=1.9-2.5$ %, then, for $x\geq 5.4\%$ the SRO parameter dramatically drops and anion distribution recovers random behavior. This SRO evolution is accompanied by a remarkable decrease in the amplitude of the FT first shell peak caused by the formation of Bi droplets at the surface, which

TABLE I. Structural parameters extracted from the fits to the XAFS data: Bi metallic fraction, ΔR, and Bi SRO parameter.

x (%)	Thickness (nm)	Bi metal fraction (%)	ΔR (Å)	Bi in second shell	Bi in second shell random	SRO parameter
1.2	270	0	0	0.00 ± 0.37	0.144	0.00 ± 2.57
1.9	210	0	0	1.12 ± 0.68	0.228	4.91 ± 2.98
2.4	210	0	0	1.11 ± 0.57	0.288	3.85 ± 1.98
5.4	38	0.49 ± 0.03	0.011 ± 0.008	0.60 ± 0.33	0.65	0.93 ± 0.51
7.0	360	0.34 ± 0.03	0.012 ± 0.005	0.40 ± 0.25	0.84	0.48 ± 0.30
8.2	38	0.52 ± 0.03	0.010 ± 0.007	0.98 ± 0.43	0.98	0.99 ± 0.44
10.9	38	0.56 ± 0.05	0.017 ± 0.020	2.47 ± 1.20	1.308	1.89 ± 0.92

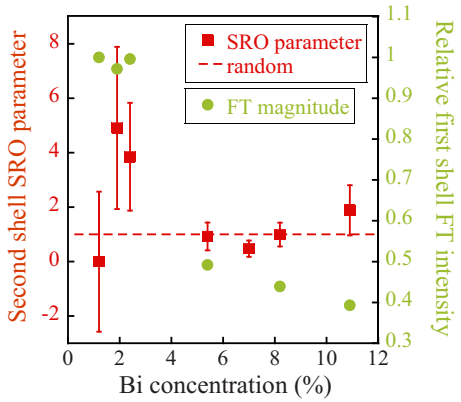

FIG. 4. (Color online) Second shell SRO parameter and relative amplitude of the XAFS FT first shell peak as a function of x.

XAFS signal overlaps the one of the epilayer. The association of the metallic contribution observed by XAFS to the Bi droplets is supported by AFM images and by the observation of a smaller FT amplitude reduction and metallic fraction in the thickest epilayer, where the surface contributes less to the XAFS signal. We note that the last point at $x=10.9\%$ matches the random value only at the limit of its error bar: this can be due to the not good agreement of the fit with data for this sample; in fact, if we exclude the FT first shell peak, the other ones are dramatically dumped here and testify an increasing structural disorder in Bi local environment, similar to the one observed in amorphous or nanostructured semiconductors.[15,16] Our results are compatible with a growth process in which, progressively increasing x, first Bi atoms tend to gather round maintaining their V-group position, then, when the tendency toward segregation becomes stronger, Bi atoms prefer aggregating into droplets at the surface and anion distribution in the epilayer recovers random character. After the SRO breaking point, the density of Bi droplets increases only weakly, and the increase in surface damage observed by AFM can be due to the formation of Ga droplets (to which Bi-edge XAFS is not directly sensitive) or semiamorphous/nanostructured areas in the sample. As a matter of fact, scanning electron microscopy and energy-dispersive x-ray analysis[17] suggest three possible compositions for the surface droplets: they can be either Bi droplets or Ga droplets or composite of Bi and Ga. In the last case, droplets are phase separated into a Ga part and a Bi part with a rather clear interface between these two. These results give an indication that droplets are not an alloy of Ga and Bi.

It is possible to establish a correlation between these structural results and the anomalous optical and electronic properties recently reported for the same samples. It has been shown that PL intensity has a nonlinear trend as a function of x: it increases with x up to values of about 4% and then dramatically drops for $x \geq 6.0\%$ while PL width reaches the maximum value in correspondence of the highest intensity.[5] As for the electronic and transport properties, very recent magneto-PL results[9] indicate that the exciton reduced mass increases counterintuitively from the dilute limit to $x=2.0\%$ and drops below the GaAs values for $x \geq 8.0\%$. The anomalous increase in exciton reduced mass and PL intensity in the low-x range roughly corresponds to the region where we observe SRO while the recovery of "usual" properties goes in parallel with the loss of SRO and the restoration of random anions distribution. Moreover, the increase in PL width for the highest PL intensity speaks for the coexistence of different Bi local environments in the most efficient samples.[10] Considering also the strong dependence of the electronic structure and carrier effective mass on the impurity distribution predicted for $GaSb_{1-x}N_x$,[11] we believe that the formation and vanishing of Bi SRO is at the origin of the unusual properties of $GaAs_{1-x}Bi_x$. An option to explain the decrease in PL intensity for $x \geq 6.0\%$ might be the presence of internal strain in the high-x epilayers due to the strongly perturbed surface,[18] nevertheless the very good quality of the XRD curve for the $x=8.2\%$ sample (Fig. 3) persuades to think that PL comes from the ordered part of the sample.

To conclude, we have given evidence of a nonlinear trend of SRO in $GaAs_{1-x}Bi_x$ as a function of x. SRO is present in the low-x range, but dramatically vanishes for $x \geq 5.4\%$, following the nonlinear behavior of optical and electronic properties. The recovery of random anion distribution for $x \geq 5.4\%$ is accompanied by formation of Bi droplets at the sample surface. The present results indicate that the increase in SRO, provided Bi surface segregation into droplets being avoided, is beneficial for the emission efficiency, which is important information for sample growth optimization. Moreover, they clarify the different steps of surface damaging and establish an evident connection between structural and emission properties. Finally, the interpretation of the alloys properties based on these results indicates that a better quantitative control and optimization of SRO degree would be an important step for compromising between emission and transport properties in the view of the utilization of dilute bismides in photovoltaic and optoelectronic devices.

We acknowledge the ESRF for funding through the Project No. MA778-MA1045, and M. Chorro for assistance.

*gianluca.ciatto@synchrotron-soleil.fr

[1] IEA, Key world energy statistics, 2009, www.iea.org
[2] J. F. Geisz and D. J. Friedman, Semicond. Sci. Technol. **17**, 769 (2002).
[3] K. W. J. Barnham *et al.*, Nature Mater. **5**, 161 (2006).
[4] T. Tiedje *et al.*, Int. J. Nanotechnol. **5**, 963 (2008).
[5] X. Lu *et al.*, Appl. Phys. Lett. **95**, 041903 (2009).
[6] A. Janotti *et al.*, Phys. Rev. B **65**, 115203 (2002).
[7] D. G. Cooke *et al.*, Appl. Phys. Lett. **89**, 122103 (2006).
[8] X. Lu *et al.*, Appl. Phys. Lett. **92**, 192110 (2008).
[9] G. Pettinari *et al.*, Phys. Rev. B **81**, 235211 (2010).
[10] G. Ciatto *et al.*, Phys. Rev. B **78**, 035325 (2008).
[11] A. Lindsay *et al.*, Phys. Rev. B **77**, 165205 (2008).
[12] G. Ciatto *et al.*, Phys. Rev. B **75**, 245212 (2007).
[13] D. J. Sprouster *et al.*, Phys. Rev. B **81**, 155414 (2010).
[14] A. Witkowska *et al.*, J. Alloys Compd. **401**, 135 (2005).
[15] M. C. Ridgway *et al.*, Phys. Rev. B **61**, 12586 (2000).
[16] L. L. Araujo *et al.*, Phys. Rev. B **74**, 184102 (2006).
[17] T. Tiedje (private communication).
[18] B. Gilbert *et al.*, Science **305**, 651 (2004).